



Contents lists available at SciVerse ScienceDirect

Surface Science

journal homepage: www.elsevier.com/locate/susc

Role of the substrate dynamics: Iron clusters deposited on an iron slab

Rafael I. González^a, Griselda García^b, Ricardo Ramírez^b, Miguel Kiwi^{b,*}^a Facultad de Física, Universidad Católica de Chile, Casilla 306, Santiago 782-0436, Chile^b Facultad de Física, Universidad Católica de Chile, Casilla 306, Santiago, Chile 7820436 and Centro para el Desarrollo de la Nanociencia y la Nanotecnología, CEDENNA, Avda. Ecuador 3493, Santiago 9170124, Chile

ARTICLE INFO

Article history:

Received 23 May 2011

Accepted 11 August 2011

Available online 22 August 2011

Keywords:

Phase transition in clusters

Cluster configuration

Cluster stability

ABSTRACT

The deposition of iron clusters on an iron substrate is investigated by means of classical molecular dynamics. The substrate dynamics is incorporated and shown to be a relevant ingredient, which leads to substantial changes of the transition temperatures, and of the thermodynamics of the cluster substrate interacting system. Fe₅₅ clusters on Fe (110) and (111) reconstructed surface orientations were studied, showing a stronger effect of the substrate dynamics for the (111) orientation. In fact, the melting temperature for a free Fe cluster, obtained by molecular dynamics simulations, is of the order of 1000 K, significantly lower than the 1812 K of bulk iron. When supported on a rigid Fe substrate it corresponds to ≈ 1400 K on both the (110) and (111) orientations. However, when the substrate dynamics is incorporated, the melting temperature changes markedly to ≈ 1200 K on the (110), and to ≈ 900 K on the (111), Fe substrate orientation.

© 2011 Elsevier B.V. All rights reserved.

1. Introduction

Cluster melting has become a subject of interest lately, both for experimentalists [1–9] and theorists. Theorists have employed several techniques, like Monte Carlo [10,11] and molecular dynamics (MD) to investigate the subject. The MD calculations have been performed both using binary potentials, like Lennard–Jones [9,12–14], and also with more sophisticated many body ones [11,15–18]. For example, Vervisch et al. [19] investigated the equilibrium structures of Pd on a MgO substrate, using a semi-empirical potential for the metal bonding within the cluster, and a potential fitted to ab initio calculations for the metal–oxide interaction. Cheng et al. [11] later on studied the thermal evolution of Pd and PdPt clusters on the same substrate.

However, to the best of our knowledge, all the studies so far have assumed the substrate to be rigid, i.e. with the substrate atoms at their zero temperature equilibrium positions. The main purpose of this contribution is to investigate the changes in the thermal evolution of clusters deposited on a substrate that result from the incorporation of the substrate dynamics in the description of the system. In particular, we are interested in the changes of the cluster melting process due to the supporting slab dynamics. Since our main concern are the changes due to the additional dynamics we have not tried to adjust the potential parameters to obtain precise values for the actual melting temperatures, but rather we have focused our attention on how these temperatures shift when the substrate dynamics is taken into consideration. To keep the physics as simple as possible we chose as our system several

different 55 atom iron clusters deposited on two reconstructed faces of bulk iron: (110) and (111). This way the evolution of the system does not depend on different inter-atomic potentials, but just on interactions among Fe atoms.

This paper is organized as follows: after this introduction in Section 2 we define the system and provide details on how the molecular dynamics is implemented. In Section 3 the results for free Fe₅₅ clusters are given, and in Section 4 the consequences of including a supporting substrate, both with and without substrate dynamics, are presented. Two different slab surfaces: (110) and (111) are studied and compared. Finally, Section 5 closes the paper with a brief summary and the relevant conclusions that we obtain.

2. System and computational methods

The system we study is composed by different shape Fe₅₅ clusters deposited on an Fe slab that acts as a substrate. We consider two crystalline orientations of the slab surface: (110) and (111). For the (110) orientation the slab consists of 8 iron monolayers, with 330 atoms each, which makes a total of 2695 atoms for the cluster plus slab system. The (111) slab consists of 24 iron monolayers of 224 atoms each, making a total for the system of 5431 atoms. Periodic boundary conditions parallel to the free slab surface are adopted.

For the interaction between the Fe atoms we adopt the potential put forward by Ackland et al. [20]. The total energy U of the system is given by

$$U_{tot} = \frac{1}{2} \sum_{ij} V(r_{ij}) - \sum_i F_i \left(\sum_{i \neq j} \rho(r_{ij}) \right), \quad (1)$$

* Corresponding author. Tel.: +56 2 354 4476.

E-mail address: mkiwi@uc.cl (M. Kiwi).

where $V(r_{ij})$ is the pair potential between Fe atoms i and j . The argument $\rho(r_{ij})$ corresponds to the electronic density due to atom j at the site of the atom located at r_i , and $F_i(\sum_{i \neq j} \rho(r_{ij}))$ is the embedding function. All the parameters, required to fully specify the interaction potential and the energy, can be found in the publication by Ackland et al. [20].

The MD simulations were carried out using a modified version of the code by Ercolessi [21,22]. The modifications we introduced allow the code to accept many body potentials of the embedded atom type [23]. The equations of motion were integrated by means of a fifth order predictor–corrector algorithm with a 1 femtosecond time step. The computations were carried out for 200 000 time steps (0.2 ns) in order to make certain that convergence had been reached. The temperature was controlled by the velocity rescaling scheme put forward by Hoover [24].

For the slab we adopted a bcc crystal structure with a 2.85 Å lattice parameter, and for the Fe₅₅ cluster four different conformations were investigated in order to determine if the initial choice is relevant for the evolution of the system towards equilibrium. These four conformations, illustrated in the upper panel of Fig. 1, are two Fe₅₅ icosahedra rotated one relative to the other by 90° (ico1 and ico2), and two rather arbitrarily cut out sections of bulk Fe (c1 and c2). The configuration c1 corresponds to a half sphere and c2 to an elongated ellipsoid. The cluster and the slab were first relaxed separately, and finally after the cluster is deposited and interacts with the slab, the system was relaxed once again. The (110) and the (111) crystal orientations were chosen in view of the abundant previous theoretical [25–27] and experimental work [28–30] available for them. Moreover, the (110) face is quite stable and its interlayer separation in the vicinity of the surface is very close to the bulk one. Actually, the reported interplanar distance difference relative to the bulk [25] is less than 3%. The structure was relaxed at 300 K during 0.1 ns and we obtained a contraction of the interplanar distance in the vicinity of the surface of just 0.25% relative to the bulk. When heating up to 1500 K this relative contraction varied only slightly. For the (111) orientation the relaxation of the interlayer distances of the slab itself is significantly larger than that for the (110) orientation, and are given in Table 1. These values are in reasonable agreement with the experiment except for d_{12} , the distance between the surface and the first subsurface layer. It is worth noticing that the (111) interlayer distances are significantly smaller than for the (110) orientation,

Table 1

Interlayer distance d_{ij} in Å units for Fe (111) and (110) oriented slabs at 300 K. Experimental results [25] are denoted by exp. The subscript 1 labels the slab surface.

Surface	d_{ij}^{exp}	d_{ij}^{MD}
(111)		
d_{12}	0.70 ± 0.03	0.806
d_{23}	0.75	0.762
d_{34}	0.86	0.878
d_{45}	0.81	0.807
d_{bulk}	0.82	0.820
(110)		
d_{12}	2.04 ± 0.04	2.014
d_{bulk}	2.02	2.02

which implies a more open surface that brings about significant consequences for the dynamics of the melting process.

3. Free Fe clusters

As mentioned above we first study the thermal evolution of free Fe₅₅ clusters. The four configurations on the upper panel of Fig. 1 correspond to two magic number full shell icosahedral configurations (ico1 and ico2) rotated, one relative to the other by 90°, and to two 55 atom clusters cut out from bulk iron (c1 and c2). Once they are heated up to 1200 K and cooled back down to 20 K all of them adopt the nearly icosahedral structures illustrated in the lower panel of Fig. 1. Thus, the initial configuration of the cluster is quite irrelevant as far as the dynamics of the melting process is concerned. The evolution of the total energy E as a function of temperature T , both for increasing and decreasing temperatures between 20 and 1200 K, is illustrated in Fig. 2. The temperature was increased and decreased in 20 K steps and the cluster was relaxed during 0.2 ns at each MD temperature step. While heating up to $T \approx 680$ K a smooth linear relation between E and T holds. Between 680 and 740 K fluctuations appear, and eventually a melting like transition is observed, with a characteristic discontinuity and a change of slope [31] of E vs. T at 740 K. The perfect matching of the energy during the cooling process of the three conformations suggests that the icosahedral configuration is a minimum energy one.

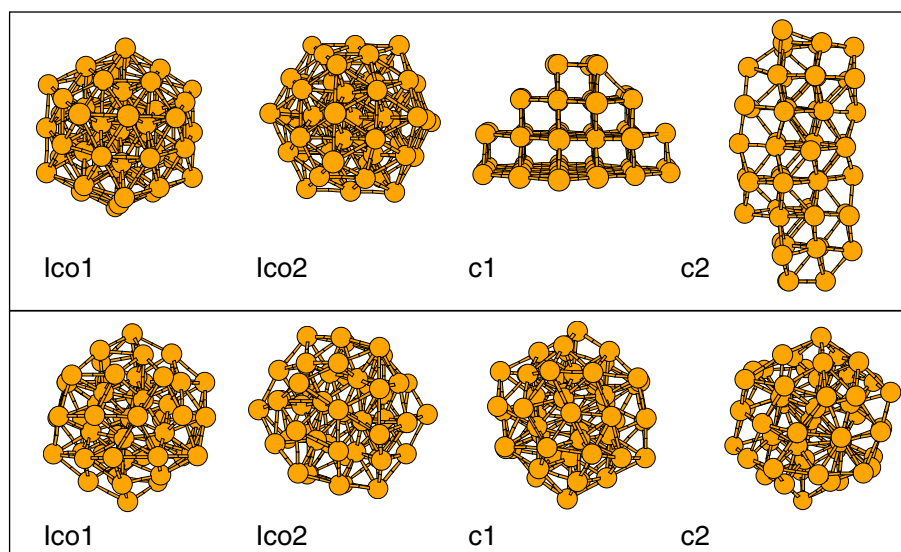


Fig. 1. Configurations of the free Fe₅₅ iron clusters we investigate. The upper panels correspond to the initial ones and the lower panels to the same after being heated to 1200 K and cooled back to 20 K.

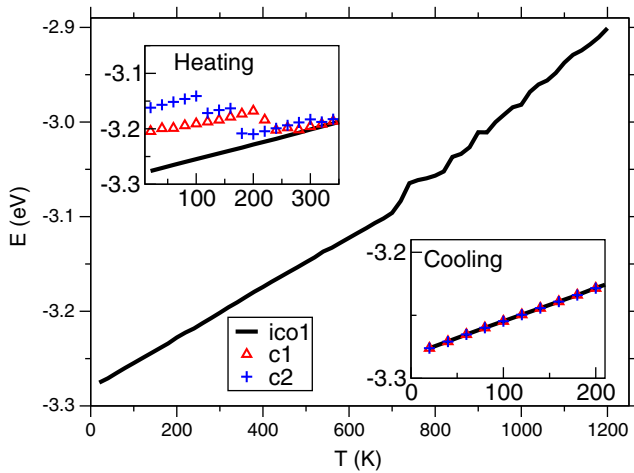


Fig. 2. Total energy vs. temperature for the free Fe_{55} clusters illustrated in Fig. 1. The main plot (continuous line) illustrates the identical heating processes of ico1 and ico2. The upper left inset illustrates the initial stages of the heating process of the configurations c1 and c2 illustrated in Fig. 1. The lower right inset depicts the close matching of the energy values during cooling for the four conformations.

In order to quantify more precisely the information of the E vs. T plot in Fig. 2, the Lindemann index [32] δ_i , and the average Lindemann index δ_c , defined as follows:

$$\delta_i = \frac{1}{N-1} \sum_{j \neq i}^N \frac{\sqrt{\langle r_{ij}^2 \rangle_T - \langle r_{ij} \rangle_T^2}}{\langle r_{ij} \rangle_T}, \quad (2)$$

and

$$\delta_c = \frac{1}{N} \sum_{i=1}^N \delta_i, \quad (3)$$

are also computed. The mean square displacement MSD is an additional useful magnitude to describe the behavior of our system. It is defined as

$$\text{MSD} = \left\langle \left| \vec{r}(t) - \vec{r}(t_0) \right|^2 \right\rangle, \quad (4)$$

where r_{ij} is the distance between cluster atoms i and j , and $\vec{r}(t)$ is the position of an atom at time t .

The values computed for the Lindemann index δ_c and the MSD as a function of temperature, for the icosahedral Fe_{55} cluster, are displayed in Fig. 3. Both experiments and simulations suggest [33,34] that values of δ_c larger than 0.1 to 0.15 constitute a reasonable criterion to establish that the system has undergone a transition to a liquid phase. Moreover, these plots are completely consistent with the data displayed in Fig. 2, since around 720 K an increase in mobility is observed, followed by a clear cut abrupt increase of both δ_c and MSD at 740 K. For $740 < T < 1000$ the Lindemann index δ_c , just as the E vs. T plot above, displays strong fluctuations as the cluster successively adopts a variety of shapes, a typical behavior of a small system in the vicinity of a transition. The smooth linear behavior of δ_c above 1000 K suggests that the cluster has become completely liquid. This transition to a quasi-molten phase, followed by a transition to a liquid, has already been observed both experimentally [1] and theoretically [14,15,35–38]. Nevertheless it is quite clear that, as expected, the free cluster turns liquid well below the 1812 K bulk iron melting temperature.

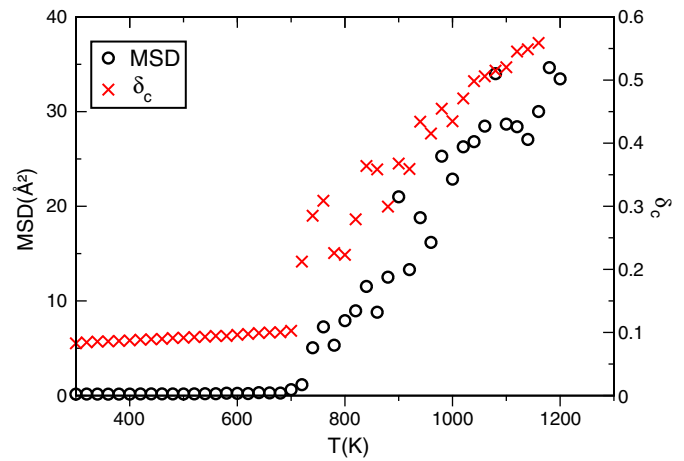


Fig. 3. Average Lindemann index δ_c (red crosses) and mean square displacement MSD (open circles) for the free ico1 Fe_{55} cluster during the heating process.

4. Cluster substrate interaction

4.1. (110) slab surface

We now turn our attention to the full system, that is, a cluster interacting with the substrate. First we relax separately the Fe_{55} clusters and an Fe (110) slab substrate, during 0.2 ns at 300 K. Next, we locate the cluster at a distance from the substrate large enough to make the cluster–slab interactions negligible. Finally, a tiny velocity is given to the cluster so that it approaches orthogonally the slab surface. Since the substrate temperature is kept fixed at 300 K most of the kinetic energy gained by the cluster, as it approaches the slab, is transferred to the latter and then dissipated into a heat bath. The process is illustrated in Fig. 4, where A corresponds to the initial stage, B to the collision, C to the atomic rearrangement and D to the epitaxial ordering of the cluster on the substrate. These results are similar to those obtained by Cheng et al. [11], who used Monte-Carlo techniques to describe the deposition of pure Pd and Pd–Pt binary clusters on a rigid MgO substrate, and also observed that the cluster adopts an epitaxial configuration with atomic layers parallel to the substrate.

The total energy E vs. T , both for the system with the substrate frozen and with dynamics, is given in Fig. 5. The slab dynamics was simulated in such a way that the bulk properties are not completely ignored; therefore, of the 8 atomic layers parallel to the slab surface, we froze half of them keeping the Fe bcc bulk structure, but allowed the atoms in the four layers closest to the cluster–slab interface to vibrate according to the temperature of the system. We observe that for temperatures below 1200 K this makes no difference, but above that T -value allowing the substrate to oscillate significantly increases E , which implies that a different equilibrium configuration is reached.

In order to provide a quantitative tool that focuses on the cluster structural changes we compute the energy difference $\delta E(T)$, that is directly related to these changes [37]. It is given by

$$\delta E = E - E_{ref} - 3(N-1)k_B T, \quad (5)$$

where E is the total energy of the system at the temperature T , E_{ref} determines the energy origin with a fixed reference value and $3(N-1)k_B T$ is the harmonic contribution. This way the potential energy of the substrate, which is large and varies only slightly with T , is omitted and consequently the variations of δE reflect the morphology of the cluster on the rigid substrate, especially the abrupt changes it undergoes. A plot of δE and the MSD vs. T is given in Fig. 6, both for the substrate without (left) and with (right) dynamics. It is of interest

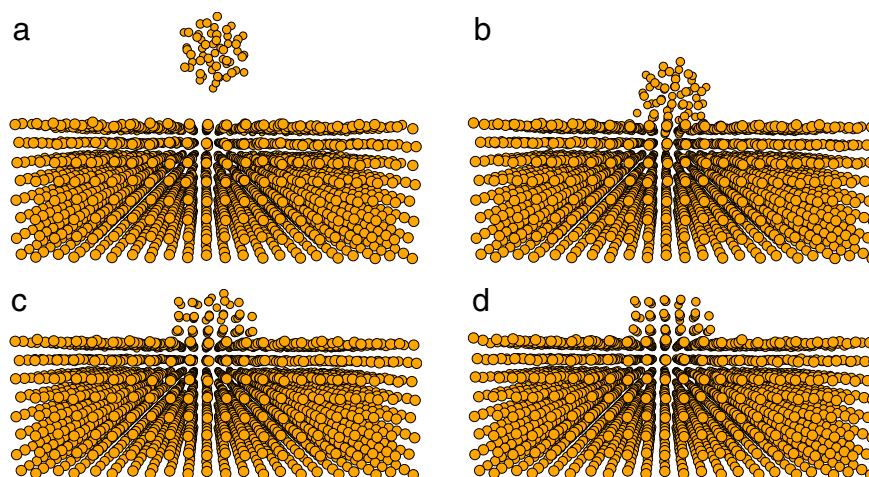


Fig. 4. Dynamics of the deposition process of an Fe_{55} cluster on the Fe (110) face of an Fe slab at 300 K. a corresponds to 0 fs, b to 8000 fs, c to 30000 fs and d to 70000 fs.

to identify each of the discontinuities of δE and the variations of the MSD in Fig. 6 to relate them to the structural changes that occur as the temperature of the system varies. The first feature we notice is that there is a substantial difference between incorporating (right) or ignoring (left) the slab dynamics. In fact, every accident in the δE vs. T plot is related to some sort of atomic rearrangement, but we limit our discussion to the major events observed in Fig. 6. In fact, the ico1 cluster, which initially has an epitaxial configuration, at 900 K loses its third layer on a dynamic slab (see panel D of Fig. 4) and becomes a two layer cluster as illustrated in Fig. 7. The analogous transition is also observed for the same cluster on a rigid slab, but at 1060 K. Therefore, the substrate dynamics reduces by 160 K the temperature required for this first atomic rearrangement. Finally, at 1040 and 1360 K, the cluster forms an additional monolayer on the substrate in both cases. Again a restructuring temperature shift of no less than 300 K is observed, due mainly to the substrate dynamics. Moreover, by inspection of the coordinates normal to the substrate surface above 980 K one observes some atomic interchange between cluster and slab (Table 2).

The substantial increase of δE observed around 1200 K in Fig. 6, for the substrate with dynamics, is best understood by inspection of Fig. 8, where we plot the average position $\langle z \rangle$ vs. the Lindemann index for ico1. The distance z is orthogonal to the slab surface, and is measured relative to the last frozen layer of the slab. Thus, for the

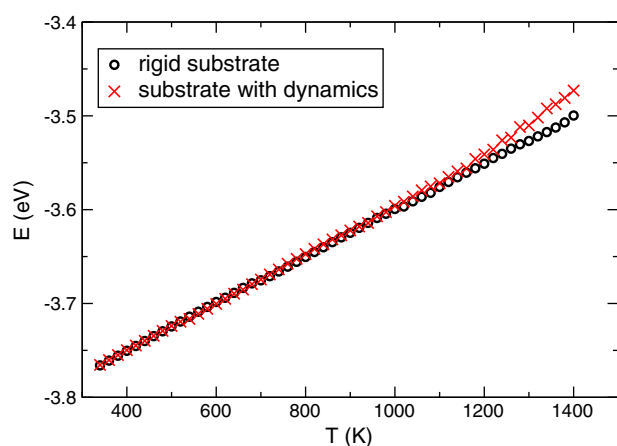


Fig. 5. Evolution of the total energy of the system consisting of an Fe_{55} cluster on the (110) surface of an Fe slab, both with (red crosses) and without (open black circles) substrate dynamics. The heating was performed at a rate of 20 K every 0.2 ns.

atoms with dynamics $z > 0$. The four substrate layers are located around $z \approx 2, 4, 6$ and 8 \AA and the cluster atoms have larger z values. At 900 K the cluster has just two monolayers and the substrate limited mobility. At 1100 K the cluster has become a monolayer and the substrate atoms display an increased mobility. At 1200 K we observe the onset of mobility of substrate subsurface atoms. In addition, some of the atoms have $\langle z \rangle$ values in between the substrate surface and the cluster, indicating that cluster–substrate atom exchange is present. This phenomenon is significantly enhanced at 1400 K, accompanied by an overall mobility increase. Consequently, the significant δE increase at 1200 K constitutes an indication that melting, from the surface towards the substrate interior, starts to take place. This increase of δE is observed only above 1400 K for a rigid substrate.

4.2. (111) oriented slab

We now present the results obtained for the dynamics of an icosahedral Fe_{55} cluster interacting with a (111) oriented Fe slab, and compare these results with those obtained for the (110) case outlined above in 4.1. Due to the fact that the initial cluster structure does not seem to make a significant difference we now limit our attention to the deposition of an icosahedron. The procedure implemented to setup the system is identical to the one specified at the beginning of 4.1. The quasi-epitaxial configuration of the system at 300 K is illustrated in Fig. 9 where one observes that the substrate crystal planes are replicated by the cluster.

The MSD of the Fe_{55} cluster deposited on the (111) slab, with and without substrate dynamics, is illustrated in Fig. 10. It is noticed that for the frozen substrate the MSD, while showing variations in magnitude, does not increase significantly below 1200 K. But, incorporating the slab dynamics leads to a clear-cut increase in mobility around 900 K, above which the atoms diffuse as in a liquid. This behavior is consistent with the δE vs. T plots of Fig. 10 which show an abrupt increase of δE around 900 K for the substrate with dynamics (right panel), and a slight decrease of the same parameter for the rigid slab (left panel), that corresponds to a rearrangement of the cluster atoms into a monolayer.

Inspection of Fig. 11, which illustrates the values of the average atomic displacements $\langle z \rangle$ for the (111) slab, shows a significant qualitative difference with Fig. 8, mainly the virtual disappearance of the layer structure in the vicinity of the interface accompanied by a significantly increased atomic mobility. Both for the (110) and (111) surfaces the cluster becomes a monolayer at 1300 K on the rigid substrate. However, when dynamics is introduced this changes considerably, and a large difference is observed for the temperature at which the solid to liquid transition takes place, which is reduced to

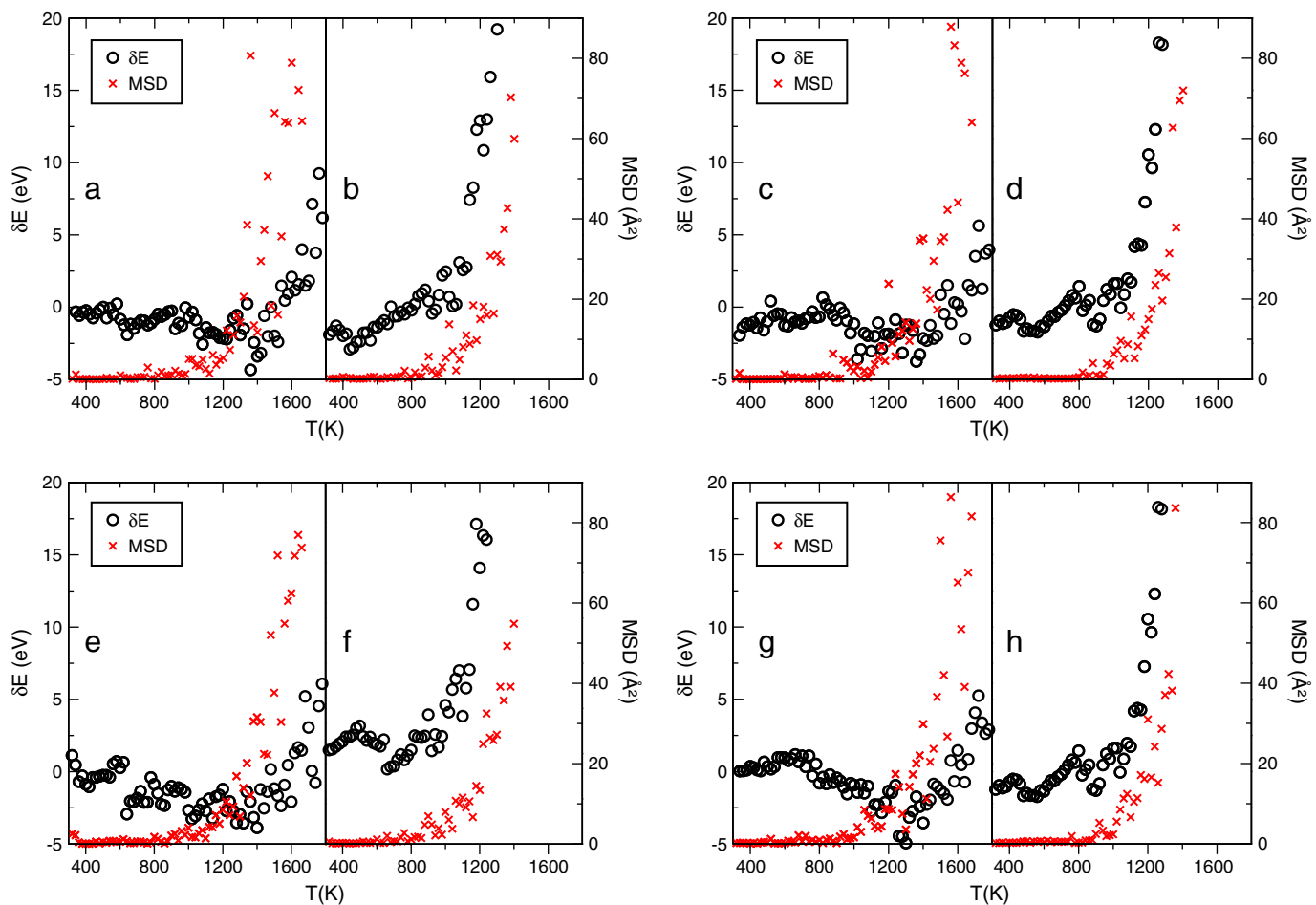


Fig. 6. Thermal evolution as described by δE and MSD for the four conformations. They correspond to: ico1 (a and b), ico2 (c and d), c1 (e and f) and c2 (g and h). On the left (right) the results without (with) substrate dynamics.

1200 K for the (110), and to 900 K for the (111), orientations. Further examination of Fig. 11 shows that the upper (111) substrate layers acquire an increased mobility already at 700 K accompanied by a cluster–substrate atomic interchange, which for the (110) orientation does not start until 1100 K are reached. Moreover, at 900 K the three layers closest to the slab surface become mobile, while the cluster keeps its layer configuration. All in all the atomic mobility of the

Table 2

Transitions and melting temperatures T_m in K for the four conformations (ico1, ico2, c1 and c2). On the left (right) without (with) substrate dynamics. For the rigid structure no melting occurs below 1400 K.

No. of layers	ico1	ico2	c1	c2	ico1-MD	ico2-MD	c1-MD	c2-MD
3 to 2	1060	1020	1000	1100	900	880	920	940
2 to 1	1360	1360	1300	1260	1040	1040	1100	1080
T_m	1400	1400	1400	1400	1160	1180	1160	1180

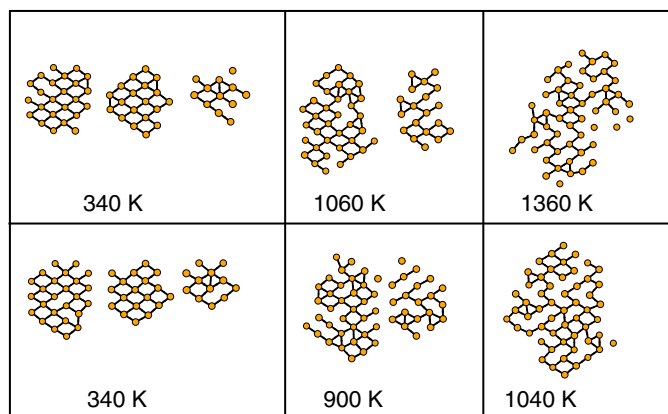


Fig. 7. Evolution of the topology of the cluster monolayers as a function of temperature, with (upper panels) and without (lower panels) dynamics. The effects due to the substrate dynamics on the magnitude of the temperature at which rearrangements occur are quite apparent.

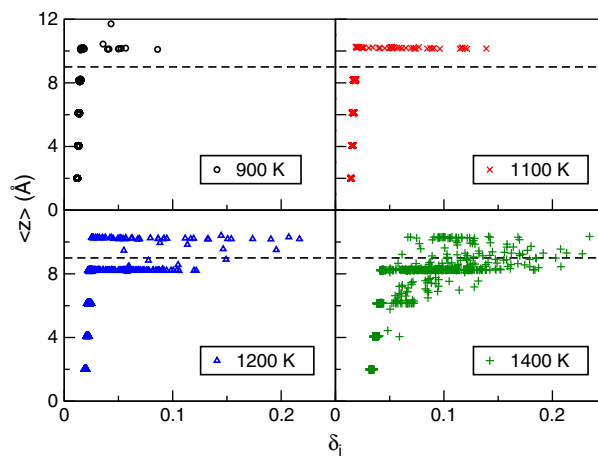


Fig. 8. Average atomic height vs. Lindemann index for all mobile atoms in the system, for the (110) oriented slab close to the cluster melting temperatures.

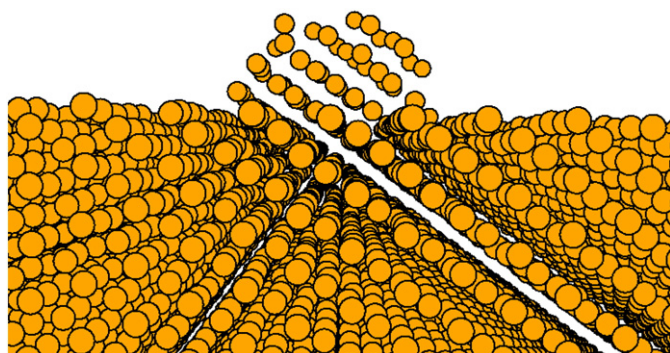


Fig. 9. Fe₅₅ deposited on an Fe (111) oriented slab at 300 K.

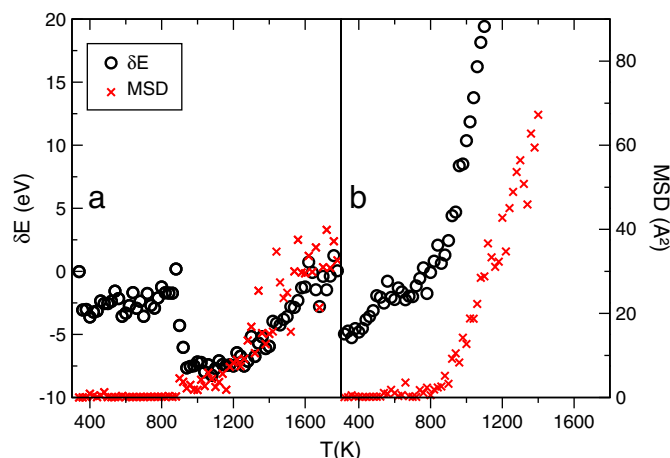


Fig. 10. Comparison between the values of δE and the MSD for an Fe₅₅ cluster on an Fe (111) slab. On the left (right) without (with) substrate dynamics.

more open (111) surface atoms reduces by 300 K the cluster melting temperature relative to the (110) orientation.

5. Summary and conclusions

In this contribution we have focused our interest on the effect of the substrate dynamics on the thermodynamics of a cluster being deposited on a surface. To keep the physics as simple as possible, and independent of the choice of binary interaction potentials, we chose as our system 55 atom iron clusters deposited on two different reconstructed faces of bulk iron: (110) and (111). The Fe cluster on an Fe substrate system was modeled by means of classical molecular dynamics and for the interaction potential we used the one put forward by Ackland [20]. Implementation of this procedure led us to the conclusion that the thermodynamics of the interacting cluster–substrate system is significantly different when the substrate dynamics is incorporated. Therefore, our results suggest trends that apply to homoepitaxial metallic systems, but these are expected to be significantly different for metallic clusters deposited on a more rigid insulating substrate, like MgO, a subject that seems worth investigating.

Both on the (110) and (111) crystallographic orientations the cluster adopted an epitaxial configuration. As the temperature was increased, from room temperature (300 K) to above 1400 K, the cluster reduces its original epitaxial configuration to just a monolayer, in discrete steps. However, the temperature values for which each of these steps takes place are substantially modified if the substrate dynamics is incorporated. In addition, the substrate surface layer does melt giving rise to interchange of atoms between cluster and substrate. For the (111) orientation the substrate dynamics induces significantly larger mobility than for (110), thus strongly lowering the cluster deposition temperature as a monolayer and its subsequent

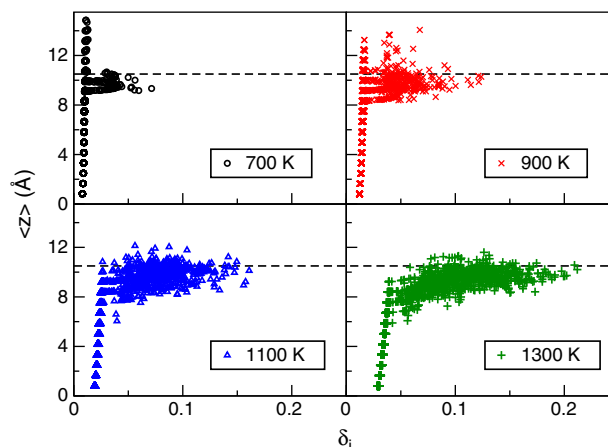


Fig. 11. Average atom height vs. Lindemann index of all mobile atoms in the system, for the (111) oriented slab near cluster melting temperatures.

melting. In fact, the reduction in transition temperatures for these processes turns out to be as large as 300 K.

In conclusion, the substrate dynamics constitutes an ingredient that should be taken into consideration when studying the melting process of clusters on a substrate.

Acknowledgment

We gratefully acknowledge stimulating conversations with Prof. José Rogan. This work was supported by the *Fondo Nacional de Investigaciones Científicas y Tecnológicas* (FONDECYT, Chile) under grants #1090225 (MK), #1080239 and #1110630 (GG and RR), and *Financiamiento Basal para Centros Científicos y Tecnológicos de Excelencia*, (GG, MK and RR).

References

- [1] P.M. Ajayan, L.D. Marks, *Phys. Rev. Lett.* 63 (3) (1989) 279.
- [2] C.R. Henry, *Prog. Surf. Sci.* 80 (2005) 92.
- [3] B. Pauwels, et al., *Phys. Rev. B* 62 (2000) 10383.
- [4] H. Hovel, *Appl. Phys. A* 72 (2001) 295.
- [5] T. Irawan, et al., *Appl. Phys. A* 80 (2005) 929.
- [6] T. Irawan, et al., *Appl. Phys. A* 82 (2006) 81.
- [7] V. Sessi, et al., *Phys. Rev. B* 81 (2010) 195403.
- [8] T. Kizuka, N. Tanaka, *Surf. Sci.* 386 (1997) 249.
- [9] P. Jensen, *Rev. Mod. Phys.* 71 (1999) 1695.
- [10] D. Cheng, et al., *Phys. Rev. B* 73 (2006) 64117.
- [11] D. Cheng, et al., *J. Phys. Chem. C* 111 (2007) 8037.
- [12] F. Ding, et al., *Appl. Phys. Lett.* 88 (2006) 133110.
- [13] E. Lamas, P. Balbuena, *J. Phys. Chem. B* 107 (2003) 11682.
- [14] J.D. Honeycutt, H.C. Andersen, *J. Phys. Chem.* 91 (19) (1987) 4950.
- [15] C. Mottet, et al., *Phase Transitions* 77 (1–2) (2004) 101.
- [16] G. Rossi, et al., *J. Phys. Chem. B* 110 (2006) 7436.
- [17] H. Dong, et al., *J. Electron. Mater.* 33 (2004) 1326.
- [18] H. Haberland, et al., *Phys. Rev. B* 51 (1995) 11061.
- [19] W. Vervisch, et al., *Phys. Rev. B* 65 (2002) 245411.
- [20] G.J. Ackland, et al., *J. Phys. Condens. Matter* 16 (2004) s2629.
- [21] F. Ercolessi, <http://www.fisica.uniud.it/~ercolessi/md/f90/2009>.
- [22] F. Ercolessi, et al., *Philos. Mag.* A 58 (1988) 213.
- [23] S.M. Foiles, et al., *Phys. Rev. B* 33 (1986) 7983.
- [24] W.G. Hoover, *Physica A* 118 (1983) 111.
- [25] M.I. Haftel, et al., *Phys. Rev. B* 42 (1990) 11540.
- [26] M. Spencer, et al., *Surf. Sci.* 513 (2002) 389.
- [27] J. Yu, et al., *Appl. Surf. Sci.* 255 (2009) 9032.
- [28] H.D. Shih, et al., *J. Phys. C* 13 (1980) 3801.
- [29] H.D. Shih, et al., *Surf. Sci.* 104 (1981) 39.
- [30] J. Sokolov, et al., *Phys. Rev. B* 33 (1986) 1397.
- [31] P. Labastie, R. Whetten, *Phys. Rev. Lett.* 65 (1990) 1567.
- [32] F. Baletto, R. Ferrando, *Rev. Mod. Phys.* 77 (1) (2005) 371.
- [33] J.H. Bilgram, *Phys. Rep.* 153 (1987) 1.
- [34] H. Lowen, *Phys. Rep.* 237 (1994) 249.
- [35] S. Alavi, D.L. Thompson, *J. Phys. Chem. A* 110 (2006) 1518.
- [36] N. Wang, et al., *Nanotechnology* 19 (2008) 415701.
- [37] F. Chen, et al., *J. Phys. Chem. C* 111 (2007) 9157.
- [38] H. Duan, et al., *Eur. Phys. J. D* 43 (2007) 185.